JOURNAL OF MATERIALS SCIENCE 23 (1988) 3113–3119

Iron-base superalloys–a phase analysis of the multicomponent system (Fe–Mn–Cr–Mo–Nb–Al–Si–C)

H. GUPTA*, H. NOWOTNY
Institute of Materials Science and Department of Metallurgy, University of Connecticut, Storrs, Connecticut 06268, USA

F. D. LEMKEY
United Technologies Research Center, East Hartford, Connecticut 06108, USA

In the course of studies on the iron-rich multicomponent system Fe–Mn–Cr–Mo–Nb–Al–Si–C, work was concentrated on pertinent quinary and six-component combinations namely Fe–Mn–Al–Si–C, Fe–Cr–Al–Si–C and Fe–Mn–Cr–Al–Si–C which had been elaborated at 65, 72, and 80 wt% Fe. From these systems the following conclusions are obvious. Manganese acts as a strong stabilizer for the cementite carbide. Chromium and silicon, when present together prefer to occur as separate phases. However, a small portion is found as intermetallics such as $CrSi_2$ or $(Fe, Mn)_5Si_3$. Chromium seems to stabilize the iron aluminide Fe_2Al_5 which forms in a considerable amount within an alloy of nominal composition Fe(65)Mn(15)Cr(12) Al(5)Si(2)C(1) (per cent by weight). Although the Mn_3AlC carbide is, like Fe_3AlC, a perovskite carbide, manganese does not appear to favour the formation of the perovskite carbide. Because of the relatively low sintering temperature (700° C), for a large portion of the samples equilibria conditions are not always reached. Furthermore, due to this temperature, iron is in the ferritic state.

1. Studies within the Fe–Mn–Cr–Mo–Nb–Al–Si–C system

As shown by Lemkey *et al.* [1, 2] alloys in the region of 10 to 20% Mn, 10 to 20% Cr, 3% C, balance iron, consist of a duplex microstructure γ (austenite) $+ M_7C_3$ carbide and can be obtained in an aligned morphology. For improvement of phase stability, mechanical properties and increasing resistance to oxidation and sulphidation, various additions, such as molybdenum, niobium, aluminium and silicon, to candidate alloys were investigated in a fairly large scope. As already demonstrated by Graig [3], improved properties were observed on addition of small amounts of niobium and silicon. In this context it is worth mentioning that niobium in a modified Mo–Nb steel enhances the nucleation of the molybdenum-cementite, which was found to be of composition $Mo_{12}Fe_{22}C_{10}$ instead of $MoFe_2C$(ξ-phase) [4, 5]. Silicon addition was found to be a beneficial influence due to the formation of silicious thin films protecting against oxidative attack.

A first survey of the phase relationship in the pertinent multicomponent systems was made by inspection of sintered samples at 700° C along the lines previously described [1, 2]. In order to confine the number of samples in a reasonable way, isothermal (isobaric) and composition sections were studied. For manganese-free alloys, as specified by 80 wt % Fe and 12 wt % Cr, the phase distribution is represented for a sum: Al + Si + C = 8 wt% (Fig. 1). As one can see, silicides and aluminides, but no binary carbide, occur with graphite. However, the complex carbide (Perovskite carbide) forms. In addition to the phases identified here, α-Fe or α-Fe-solid solution (ferrite) and chromium are also present. At this point it is of interest to refer to the separation tendency of chromium in other superalloys (i.e. nickel-base superalloys [6]). Neither aluminium, silicon or carbon seem to diminish the separation. Thus, for example, in the carbon-free alloy (80Fe, 12Cr, 8Si), displaying α-Fe ($a = 0.286_4$ nm), Fe_3Si ($a = 0.565_1$ nm), $CrSi_2$ ($a = 0.442_1$, $c = 0.635$ nm), elemental silicon, MSi and chromium are present. The lattice parameter for chromium of 0.288_0 nm corresponds to that of pure chromium.

2. The ternary and quaternary subsystems

2.1. Fe–Cr–Al, Fe–Cr–Al–C

The ternary system is well known from studies of the Kanthal-type alloys. For a composition of 80 wt % Fe, 12 wt % Cr, 8 wt % Al the major phase is ferrite (0.286_7 nm) where some chromium and aluminium are dissolved. Furthermore, the intermetallic Fe_2Al_5 and elemental chromium is observed. With addition of carbon i.e. 80 wt % Fe, 12 wt % Cr, 1 wt % Al, 7 wt % C,

*Author to whom all correspondence should be addressed.

0022–2461/88 $03.00 + .12

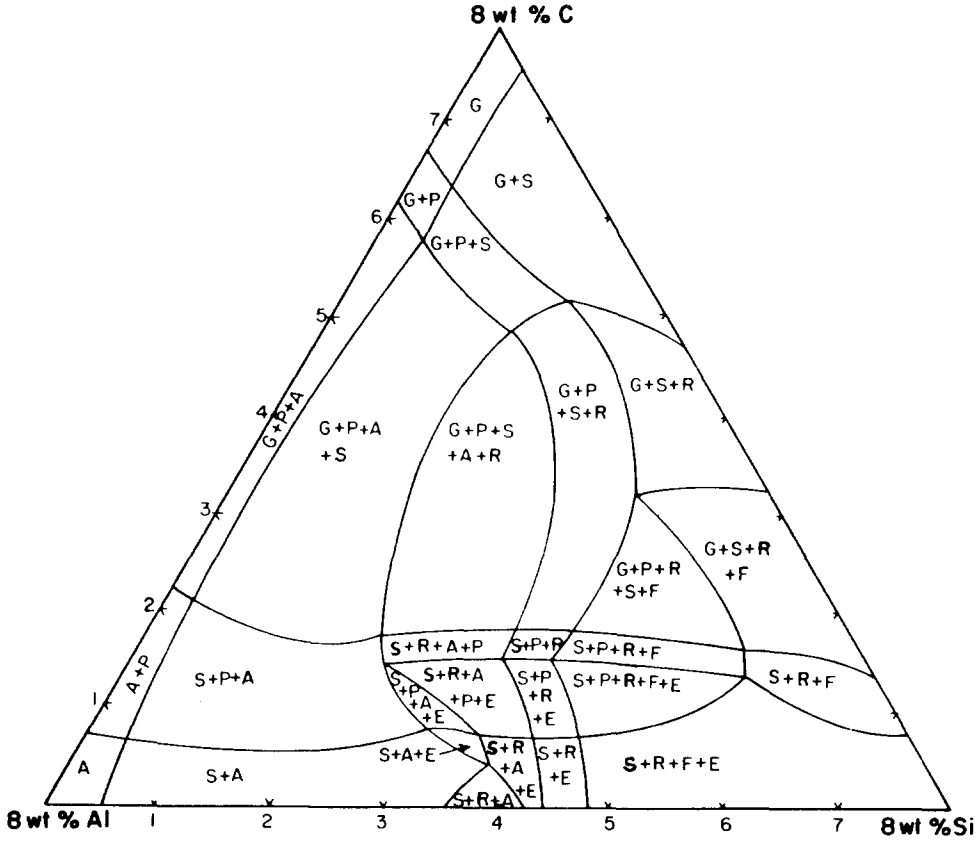

Figure 1 Fe–Cr–Al–Si–C section at 700° C, for 80 wt % Fe and 12 wt % Cr. α-Fe and chromium are present in all phase fields and hence are not shown. G, graphite; S, silicon (elemental); P, perovskite; A, iron aluminide Fe_2Al_5; R, chromium disilicide $CrSi_2$; F, iron silicide Fe_3Si; E, iron silicide FeSi.

ferrite, chromium and graphite also occur. Increasing the ratio Al/C (Table I) leads to formation of perovskite carbide and Fe_2Al_5 as demonstrated by the alloys (80% Fe, 12% Cr, 2% Al, 6% C), (80% Fe, 12% Cr, 3% Al, 5% C) and (80% Fe, 12% Cr, 5% Al, 3% C). From the evaluation of the X-ray powder pattern of alloy 80 wt % Fe, 12 wt % Cr, 5 wt % Al, 3 wt % C, a parameter of 0.379_1 nm for the perovskite carbide results. The relatively large value of 0.287_5 nm for the ferrite indicates an α-Fe(Cr, Al) solid solution is present. With respect to the perovskite carbide, a similar parameter (0.376 nm) is obtained for alloy 80% Fe, 12% Cr, 4% Al, 4% C. The slight variation in the cell parameter is due to the amount of carbon filling the interstitial sites and to the degree of order: austenite–perovskite [7].

TABLE I Selected alloys in the quinary system: 80 wt % Fe, 12 wt % Cr, 8 wt % (Al + Si + C)

Al	Si	C	Phases
			Ferrite + Cr +
3	–	5	P + Fe_2Al_5(t) + G
1	–	7	G
–	2	6	G + Si
4	1	3	P + G + Fe_2Al_5 + Si
–	6	2	$CrSi_2$ + M_3Si(t) + Si + G
2	4	2	Si + P + G + $CrSi_2$ + M_3Si
2	1	5	G + P + Si + $CrSi_2$
3	3	2	Si + P + Fe_2Al_5 + $CrSi_2$ + G
1	6	1	MSi + M_3Si + Si + $CrSi_2$
6	–	2	Fe_2Al_5 + P
6	1	1	Si + P + Fe_2Al_5

G, graphite; P, perovskite; t, trace.

2.2. Fe–Mn–Al, Fe–Mn–Al–C

The Fe–Mn–Al and Fe–Mn–Al–C systems have drawn attention recently with regard to development of duplex microstructures γ/γ', after heat treatment. Iron-rich alloys such as 15 wt % Mn, 8 wt % Al, 2 wt % C, balance Fe, have recently been studied [8] in the rapidly solidified state. The authors found the lattice parameters to be: a_γ = 0.3677 nm and for $\gamma' a$ = 0.3756 nm, respectively. The perovskite carbide is named the K-phase. In order to elucidate the role of the perovskite carbide, measurements were also made on Fe–Mn–Al–C samples with increasing amounts of carbon from 1.6 to 2.4 wt % C. The γ' phase corresponds to the perovskite carbide $(Fe, Mn)_3AlC$. In fact, the γ'-phase in the analogue Ni–Al–C system has been shown to be $Ni_3Al(C)$, that means there is a small solubility in Ni_3Al for carbon [9].

From a set of alloys which were cast and annealed one can see essentially duplex structure develops for Fe–Mn–Al–C samples with 1.6 to 2.4 wt % C after annealing at 800° C for 40 h (Table II). Ferritic solid solutions only form as traces after heat treatment. Assuming a continuous transition between Fe_3AlC_x and Mn_3AlC, a lattice parameter of 0.3789 nm for a composition of $Fe_{2.15}Mn_{0.85}AlC$ results. As with many transition element carbides, carbon deficiency occurs frequently or varies within a homogeneous range. It appears, nevertheless, that for the occurrence of γ'(P) in multicomponent systems, the presence of aluminium more decisive, rather than that of manganese.

2.3. Fe–Cr–Si, Fe–Cr–Si–C

As compared to the aluminium containing systems,

TABLE II Phase analysis and lattice parameters for Fe(bal)–Mn(20)–Al(8)–C alloys; Co$K\alpha$ radiation

Carbon (wt %)	Phases	Lattice parameters (nm)
1.6 (as-cast)	major γ	$a = 0.3687_5$
	minor α	$a = 0.2867_5$
2.0 (as-cast)	major γ	$a = 0.3689$
	minor α	$a = 0.2861_0$
2.0 (820° C, 40 h)	major γ	$a = 0.3658_0$
	minor γ' (P)	$a = 0.3776_5$
	trace α	$a = 0.2867_5$
2.4 (as-cast)	major α	$a = 0.2876_0$
	minor γ	$a = 0.3707_0$

in the manganese-free combinations Fe–Cr–Si and Fe–Cr–Si–C, silicon reacts only partially in the sintered state, which can be expected from the melting points of aluminium and silicon, respectively. Within an alloy 80 wt % Fe, 12 wt % Cr, 8 wt % Si, ferrite ($a = 0.286_4$ nm), chromium (0.288_1 nm), Fe_3Si ($a = 0.565_1$ nm) and free silicon have been identified and traces of $CrSi_2$ and MSi were present. Only negligible substitution of the transition metals in the silicides except for M_5Si_3 and MSi (M = metal) can be assumed. While for an alloy 80 wt % Fe, 12 wt % Cr, 8 wt % C, all equilibria are known from the stable or metastable Fe–Cr–C systems as the best explored iron-base combination; the quaternary Fe–Cr–Si–C has been much less investigated. For these alloys the occurrence of ferrite and graphite is characteristic. In contrast to the behaviour of the M_7C_3 and $M_{23}C_6$ carbides, there is no significant Cr/Fe substitution within Cr_3C_2. Alloys having 1 to 3 wt % Si, 7 to 5 wt % C with the sum Si + C = 8 wt % exhibit, besides ferrite and chromium, graphite and free silicon.

2.4. Fe–Mn–Si, Fe–Mn–Si–C

The silicides of the Fe–Mn–Si ternary exhibit extended or complete solid solutions such as $(Fe, Mn)_3Si$ [8], $(Fe, Mn)_5Si_2$ [9], $(Fe, Mn)_5Si_3$ [10], (Fe, Mn)Si [11] and $(Fe, Mn)Si_2$ [11]. With respect to the quaternary system Fe–Mn–Si–C, a recent work on a novel high-strength steel of composition 3 wt % Mn, 1.5 wt % Si, 0.3 to 0.5 wt % C, balance Fe, shoud be mentioned [12].

3. The quinary and higher systems

3.1. Fe–Cr–Al–Si–C, Fe–Mn–Al–Si–C

The phase analysis for alloys 80 wt % Fe, 12 wt % Cr, 8 wt % (Al + Si + C) reveals the occurrence of ferrite, chromium, graphite, silicon, perovskite carbide, Fe_2Al_5, Fe_3Si and $CrSi_2$ with preference of a compositional sequence: carbon-rich, aluminium-rich, silicon-rich, Table I (Fig. 1). Inspection of alloys 72 wt % Fe, 20 wt % Mn, 8 wt % (Al + Si + C), on the other hand, shows the presence of ferrite, graphite, β-Mn type phase, M_3C (cementite) and FeSi. From this

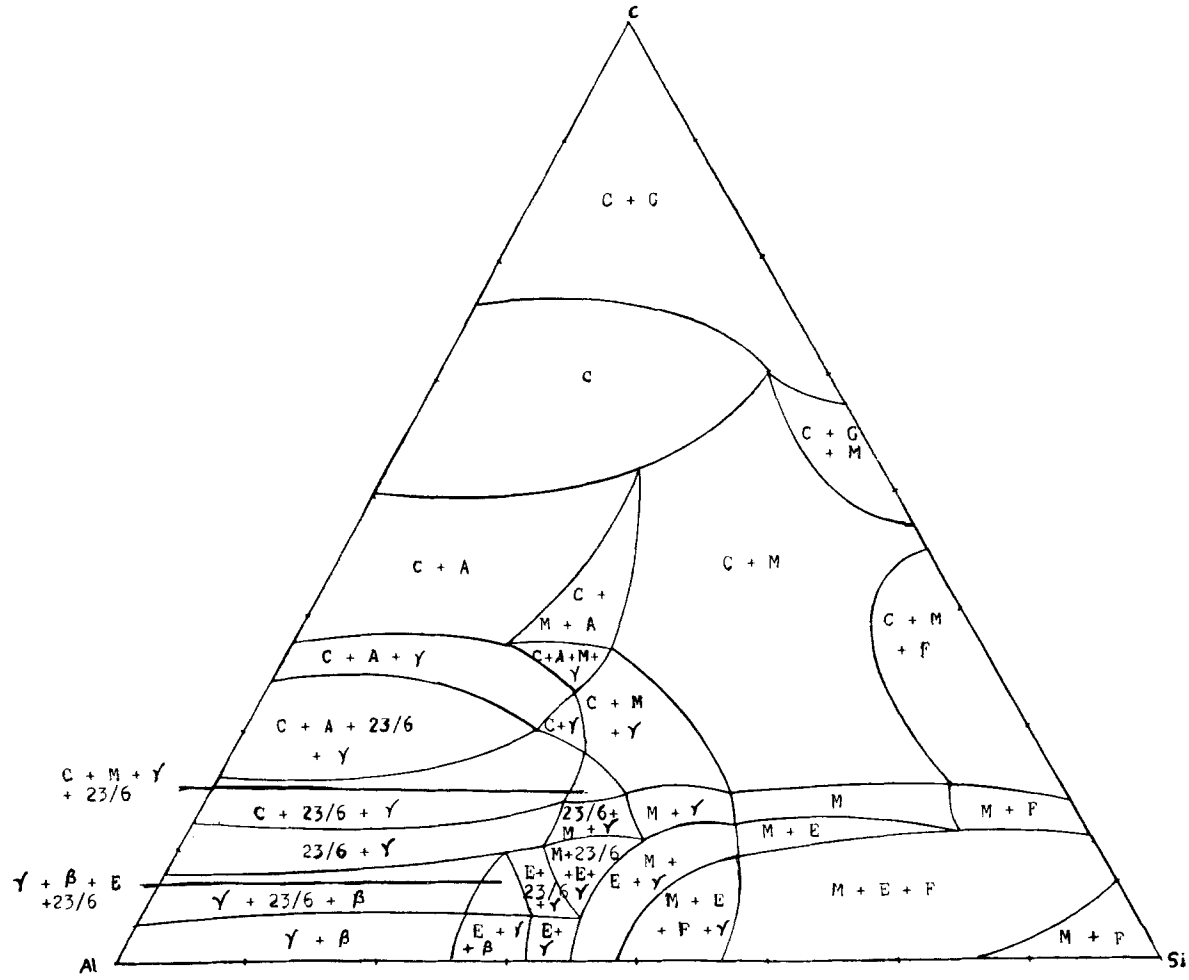

Figure 2 Fe–Mn–Al–Si–C section at 700° C, for 72 wt % Fe and 20 wt % Mn. α-Fe is present in all phase fields. C, cementite; G, graphite; M, $D8_8$–$(Fe, Mn)_5Si_3$; A, Fe_2Al_5; γ = γ-Fe; 23/6, $M_{23}C_6$ carbide; β, β-Mn; E, MnSi; F, M_3Si.

TABLE III Phase analysis for selected alloys 72 wt % Fe, 20 wt % Mn, 8 wt % (Al + Si + C)

Al	Si	C	Phases*
–	–	8	C + G
–	1	7	C + G
1	0	7	C + G
–	2	6	C + G
1	1	6	C + G
3	0	5	C
5	0	3	Fe_2Al_5 + C
2	3	3	C + $D8_8$
4	1	3	C + Fe_2Al_5
7	–	1	γ-Fe (0.3594 nm) + 23/6
6	1	1	γ-Fe (0.3587$_2$ nm) + 23/6 + C(t)
–	6	2	Fe_3Si (0.5657 nm) + C + $D8_8$
2	5	1	$D8_8$ + Fe_3Si + MSI
6	–	2	23/6 + C + γ-Fe + Fe_2Al_5
–	3	5	G + C

*α-Fe present in all alloys. C, cementite M_3C; G, graphite; t, trace.

TABLE IV A selection of sintered alloys within alloys of type 65 wt % Fe, 15 wt % Mn, 12 wt % Cr, 8 wt % (Al, Si, C)

Composition addition (wt %)			Phases*
Al	Si	C	
–	–	8	G + C
–	1	7	G + C
1	–	7	G + C
–	2	6	G + C
1	1	6	G + Si + C
3	–	5	C + 23/6 + G + A
4	–	4	C + A + 23/6 + G
3	2	3	C + Si + A
–	6	2	M + $CrSi_2$ + C + Fe_3Si
3	4	1	Si + C + $CrSi_2$
5	2	1	C + A + 23/6 + Si(t); t = trace
5	3	0	β-Mn† + Si + unid.
1	4	3	C + Si + $CrSi_2$
4	1	3	C + 23/6 + A + Si
–	4	4	C + M + G
1	5	2	M + Si + $CrSi_2$ + C + Fe_3Si
3	3	2	C + Si + $CrSi_2$ + 23/6 + A
4	2	2	C + Si + 23/6 + A

*α-Fe and Cr present in all alloys.
†β-Mn or β-Mn carbide.
M, Mn_5Si_3; A, Fe_2Al_5; C, cementite; G, graphite; 23/6, $M_{23}C_6$ carbide.

analysis Fig. 2 has been derived. It should be added, however, that traces of two unidentified constituents were neglected. The phase analysis for selected alloys with 72 wt % Fe, 20 wt % Mn and 8 wt % (Al + Si + C) is presented in Table III. From these quinary systems one can conclude that manganese is a strong stabilizer for the cementite carbide. The findings concerning the decrease of the cell size by the Fe/Mn substitution in the cementite carbide [15] have been corroborated. The lattice parameters for the substituted cementite were found to be distinctly smaller (a = 0.5076, b = 0.6722, c = 0.4515 nm) than those for pure cementite.

Chromium and silicon, when present together, prefer to occur in separate phases mainly observed in the elemental state, but a portion is found as silicides such as $CrSi_2$ or $(Fe, Mn)_5Si_3$. It appears, furthermore, that chromium stabilizes the aluminide Fe_2Al_5 which forms in a considerable amount, i.e. within a six-component alloy of nominal composition 65 wt % Fe, 15 wt % Mn, 12 wt % Cr, 5 wt % Al, 2 wt % Si, 1 wt % C. Shifting from the two quinaries to the six-component system no noticeable change of the lattice parameters in the corresponding constituents have been observed. Table IV and Fig. 3 summarize the results for the iron-rich six-component system.

Some particular observations are to be described which, in part, relate to participating components such as molybdenum and niobium. The exploration was concentrated on the analysis of alloys at 92 wt % metal (Fe, Mn, Cr, Mo, Nb) and 8 wt % (Al + Si + C). In the sintered state (700° C), α-Fe solid solution (a = 0.2865 nm) shows up with a major portion of cementite M_3C, M_2C, graphite and traces

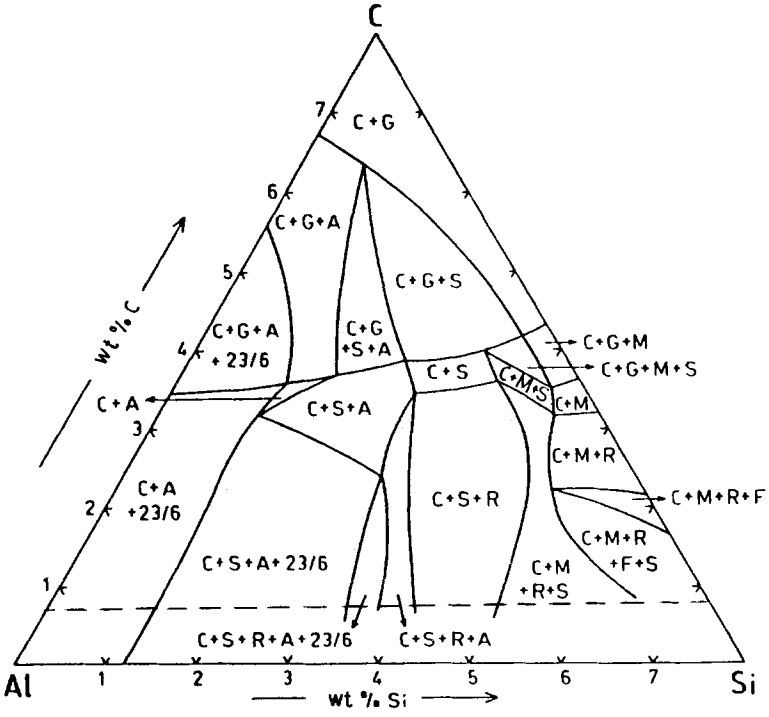

Figure 3 Fe–Mn–Cr–Al–Si–C section at 700° C for 65 wt % Fe, 15 wt % Mn and 12 wt % Cr. α-Fe and chromium are present in all phase fields. The diagram is not completed below the dotted line due to insufficient data. C, cementite; G, graphite; S, silicon; M, Mn_5Si_3; R, $CrSi_2$; F, Fe_3Si; A, Al_5Fe_2; 23/6, $M_{23}C_6$ carbide.

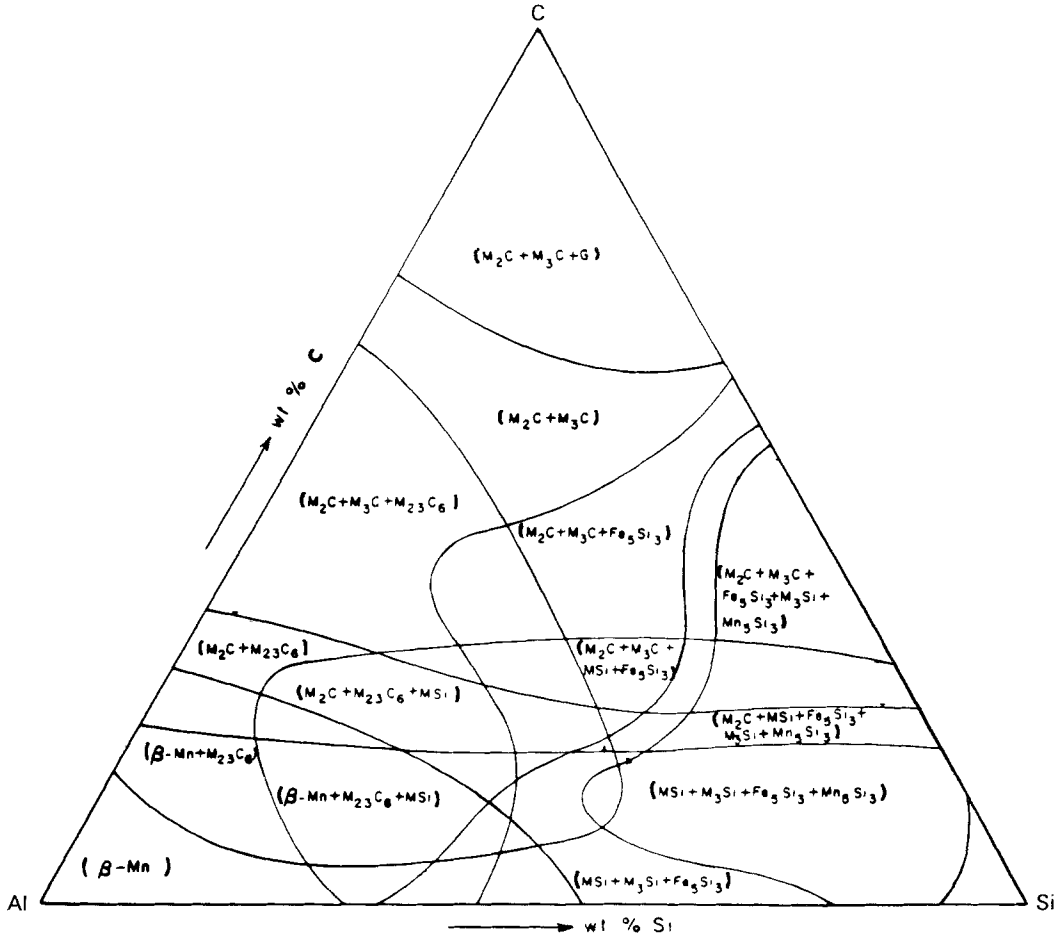

Figure 4 62 wt % Fe, 15 wt % Mn, 12 wt % Cr, 2 wt % Mo, 1 wt % Nb and 8 wt % (Al + Si + C) section at 700° C as prepared by ZPF lines.

of chromium. The lattice parameters of M_2C (a = 0.3011, c = 0.474 nm) indicate that there is more Mo/Nb rather Mo/Mn substitution. Within the boundary system Fe–Mn–Mo–C, the occurrence of the subcarbide $(Mo, Mn, Fe)_2C$ can be confirmed with arc-melted samples. Increasing the ratio Mo/Mn yields lattice parameters of the subcarbide (a = 0.2957_8, c = 0.4690_4 nm) fitting the interpolated lines for "Mn_2C"–Mo_2C at a section M_7C_3 corresponding to $Fe_{0.7}Mn_{4.2}Mo_{2.1}C_3$. The decrease in cell parameters in the subcarbide is very likely compensated by niobium as $(Mo, Nb, Mn)_2C$. The subcarbide seems to be less modified by chromium, but like manganese substitutes within cementite as $(Fe, Mn, Cr)_3C$, ignoring molybdenum.

Increasing aluminium and silicon at the expense of carbon does not change the above listed constituents, but chromium very distinctly separates out, i.e. in (62Fe, 15Mn, 12Cr, 2Mo, 1Nb, 3Si, 5C) or (62Fe, 15Mn, 12Cr, 2Mo, 1Nb, 3Al, 5C). Higher amounts of aluminium favour its solubility in ferrite as is shown for alloy (62Fe, 15Mn, 12Cr, 2Mo, 1Nb, 5Al, 3C) (a = 0.2880 nm), for example.

The silicides identified as Fe_3Si and one or two $D8_8$-type phases were found to be associated with ferrite (a = 0.287 nm), Fe_2MnSi (a = 0.566_4 nm) and $(Fe_{0.75}Mn_{0.25})_5Si_3$ (a = 0.684, c = 0.4718 nm). For instance, in an alloy of the same set with 8 wt % Si besides ferrite (a = 0.2864 nm) and free chromium, both the silicides M_3Si and M_5Si_3 appear to be present. With further increasing of the amount of aluminium the β-Mn phase begins to show up, i.e. in an alloy having 62% Fe, 15% Mn, 12% Cr, 2% Mo, 1% Nb, 8 wt % Al. Similar results are obtained from an alloy with 5 wt % Al and 3 wt % Si, in which additional M_3Si silicides are observed. As FeSi, MnSi and CrSi form continuous series of solid solutions, the monosilicide is very likely to be (Fe, Mn, Cr)Si. The MSi phase, monosilicide Fe–Mn also shows up with a = 0.455_2 nm in an alloy with 1 wt % Al, 6 wt % Si and 1 wt % C, while a carbon- and silicon-free alloy with 8 wt % Al does not display any intermetallic. This alloy consists of ferrite, a = 0.288_6 nm, chromium a = 0.291_0 nm and β-Mn phase (0.628 nm). In the β-Mn phase there is iron–manganese substitution, which accounts for the decrease of the lattice parameter from 0.6314_5 nm to the above mentioned value. The increase of the parameter for the austenitic phase is due to manganese, while the increase for the ferrite, as well as for the chromium phase mainly stems from aluminium. As found previously [1], the β-Mn phase or π-phase (with carbon) widely occurs in these systems, thus in silicon-containing alloys the parameter of the β-Mn or π-phase may even be reduced to 0.6213_5 nm. Fig. 4, which is a topological diagram, shows the phase repartition for alloys: 62 wt % Fe, 15 wt % Mn, 12 wt % Cr, 2 wt % Mo, 1 wt % Nb and 8 wt % (Al + Si + C) in the sintered state at 700° C. Note this diagram also appears in [16] as an example of the application of the overlapping zero-phase fraction line method, introduced by Gupta *et al.* Because of lack of space, some of the phase fields in this diagram are not labelled. The reader is referred to Gupta *et al.'s* article [16] for details of this diagram.

TABLE V (a) Sintered alloys at 1000° C: phase identification

Cr(20)Mn(10)C(3.3)Al(1.0)Mo(1.5) bal. Fe
Phases: M_7C_3 (a = 1.394, c = 0.449 nm)
γ-Fe (a = 0.360 nm)
Cr(15)Mn(15)C(3.3)Al(1.0)Mo(1.0) bal. Fe
Phases: as above
Cr(12)Mn(18)C(3.3)Al(1.0)Mo(1.0) bal. Fe
Phases: M_7C_3 (a = 1.394_2, c = 0.450_4 nm)
β-Mn (a = 0.6215 nm)
γ-Fe (a = 0.359_6 nm)
Cr(17)Mn(12)C(3.3)Al(1.0)Mo(1.5) bal. Fe
Phases: M_7C_3 (a = 1.3939, c = 0.450 nm)
M_2C (a = 0.300_4, c = 0.4711 nm)
γ-Fe (a = 0.3596 nm)
Cr(17)Mn(12)C(3.3)Al(1.0)Mo(1.0) bal. Fe
Phases: M_7C_3 (a = 1.3957, c = 0.4508 nm)
α-Fe (a = 0.286_7 nm)
Cr(17)Mn(12)C(3.3)Al(1.0)Mo(1.5)Nb(0.5) bal. Fe
Phases: M_7C_3 (a = 1.392_5, c = 0.4498 nm)
α-Fe (a = 0.285_6 nm)
Cr(20)Mn(10)C(3.3)Al(0.5)Mo(0.5)Si(1.0)Nb(1.0) bal. Fe
Phases: M_7C_3 (a = 1.3936, c = 0.4494 nm)
α-Fe (a = 0.285_8 nm)
Cr(17)Mn(11)C(3.4)Mo(1.5)Nb(0.5)Al(1.0)Si(1.0) bal. Fe
Phases: M_7C_3
MC (a = 0.443 nm)
γ-Fe (trace)
α-Fe (trace)
Cr(17)Mn(12)C(3.3)Mo(1.5)Nb(1.0)Al(1.0)Si(1.0) bal. Fe
Phases: M_7C_3
MC
α-Fe
γ-Fe
Cr(12)Mn(18)C(3.3)Al(1.0)Mo(1.0)Si(1.0)Nb(1.0) bal. Fe
Phases: M_7C_3 (a = 1.392_9, c = 0.4497 nm)
MC (a = 0.444_6 nm)
γ-Fe (a = 0.3603 nm)
Cr(16)Mn(14)C(3.4)Mo(1.0)Si(0.5)Nb(0.5) bal. Fe
Phases: M_7C_3 (a = 1.395_2, c = 0.450 nm)
γ-Fe (a = 0.360_3 nm)
Cr(18)Mn(14)C(3.4)Al(0.5)Mo(1.0)Si(0.5)Nb(0.5) bal. Fe
Phases: M_7C_3 (a = 1.393_6, c = 0.450 nm)
γ-Fe (a = 0.360 nm)
MC

(b) Arc-melted (AM) and sintered (S) alloys at 800° C

(63Fe, 15Mn, 12Cr, 2Mo, 5Si, 3C wt %, nominal) S-800° C
= α (a = 0.288_2 mn) + Fe_3Si (a = 0.568_0 nm)
+ trace of unidentified phase
(64Fe, 15Mn, 12Cr, 2Mo, 5Al, 2C wt %, nominal) AM
= γ (a = 0.366_0 nm) + α (a = 0.286_5 nm)
+ M_7C_3; α small amount.
(64Fe, 15Mn, 12Cr, 2Mo, 3Al, 2Si, 2C wt %, nominal) AM
= γ (a = 0.364_3 nm) + M_7C_3 + trace of unidentified phase
(64Fe, 15Mn, 12Cr, 2Mo, 3Al, 2Si, 2C wt %, nominal) S-800° C
= γ (a = 0.362_6 nm) + α (0.288_5 nm) + M_7C_3
(64Fe, 15Mn, 12Cr, 2Mo, 2Al, 3Si, 2C wt %, nominal) AM
= γ (a = 0.363_0 nm) + α (0.286_4 nm) + M_7C_3

TABLE VI Phase analysis in alloys (a) Fe(64)Mn(15)Cr(12)Mo(2)[Al, Si, C] (7), sintered (800° C)

Al	Si	C	Phases
5	–	2	γ + trace α + M_7C_3
4	1	2	α + γ + M_7C_3
3	2	2	α + M_7C_3
2	3	2	α + M_7C_3 + unident.
1	4	2	α + minor γ + M_7C_3
–	5	2	α + minor γ + M_7C_3 + unident

(b) Fe(63)Mn(15)C5(12)Mo(2)[Al, Si, C] (8) arc melted and annealed

Annealing temp. (° C)	Al	Si	C	Phases
1000	5	–	3	γ + M_7C_3 + trace α
700	5	–	3	similar to 1000° C
1000	4	1	3	α + γ + carbide
700	4	1	3	similar to 1000° C
1000	3	2	3	α + M_7C_3 + minor γ
700	3	2	3	similar to 1000° C
1000	2	3	3	α + M_7C_3 + unident.
700	2	3	3	similar to 1000° C
1000	1	4	3	α + M_7C_3 + minor γ
700	1	4	3	α + M_7C_3 + M_2C + unident.
700	–	5	3	α + minor M_7C_3 + unident.

Alloys within the system: 63 wt % Fe, 15 wt % Mn, 12 wt % Cr, 2 wt % Mo, 8 wt % (Al + Si + C) are melted and annealed at 700 and 1000° C.

Comparison between sintered (at 1000° C) and (chill) cast alloys virtually do not differ with regards to the constituents. The phase identification of sintered alloys (1000° C) is revealed by Table V. In Table VI results are presented for arc-melted samples confirming the predominance of the M_7C_3 carbide in an austenitic matrix. This also holds for sintered (1100° C) and arc melted and annealed samples. As an example, an alloy with (63Fe, 15Mn, 12Cr, 2Mo, 4Al, 1Si, 3C wt % nominal) consists of γ (a = 0.362_3 nm) and M_7C_3 (a = 1.392_8, c = 0.451_2 nm). Furthermore, molybdenum is known to favour the formation of M_2C carbide while the ratio Mn/Cr is critical for the uniformity of the γ-matrix. With respect to niobium addition, it was found that molybdenum and niobium interact so far, as competition between the M_2C and MC carbides takes place (Table V). Both these carbides form as (Nb, Mo)C and $(Nb, Mo)_2C$. These findings concerning the high carbon-containing carbides correspond, by and large, to those for the extracted carbides [17]. Because of the high stability of both these carbides there is quite a change in the phase distribution of the Fe–Mn–Cr–Mo–Nb–Al–Si–C system compared to the sintered state at 700° C. Filings of directionally solidified bars also show the duplex character. For an alloy (nominal 64.3Fe, 15Mn, 12Cr, 2.5Al, 3.2C wt %) the γ-matrix, displaying strongly distorted crystallites, has a cell parameter of a = 0.363_7 nm and the M_7C_3 carbide (a = 1.396, c = 0.4500 nm). Similar findings were obtained for analogous materials of nominal composition 64.2Fe, 15Mn, 15Cr, 2Mo, 1Si and 2.8C [18].

4. Conclusion

In attempting to develop iron-base superalloys which can meet the requirements of high strength and corrosion resistance at elevated temperature, the influence of additions proposed from the point of view of low cost and favourable with respect to low density and easy availability, yields the multicomponent system Fe–Mn–Cr–Mo–Nb–Si–Al–C. A phase analysis was preferentially carried out for alloys having 65 to 80 wt % Fe, small amounts of molybdenum (2 wt %) and niobium (0.5 wt %) and variations of Al + Si + C (8 wt %). Starting with the ternaries, a complete phase analysis of the eight-component combination reveals the complexity of the equilibria which occur. The

pronounced separation of chromium is of particular interest; furthermore manganese, essential for the austenitic matrix, was found to be acting as a strong cementite stabilizer. With respect to the formation of the perovskite carbide, aluminium is more effective than manganese. Although silicon also shows a tendency for separating, all the expected silicides form mainly as solid solutions with the corresponding iron silicides. The additions of molybdenum and niobium are clearly visible in the formation of the highly stable mono- and subcarbides as solid solutions (Nb, Mo)C and $(Mo, Mn, Fe)_2C$. Other predominant complex carbides are the π-phase, previously described, and the M_7C_3 carbide [1]. The results now allow additions of molybdenum, niobium, aluminium and silicon to be minimized for Fe–Mn–Cr–C base superalloys in order to maintain the pertinent constituents.

Acknowledgement

The authors gratefully acknowledge the support of NASA Lewis Research Center under the COSAM project, grant NAG3-271.

References

1. F. D. LEMKEY, H. GUPTA, H. NOWOTNY and S. F. WAYNE, *J. Mater. Sci.* **19**(1984) 965.
2. F. D. LEMKEY, E. R. THOMPSON, J. C. SCHUSTER and N. NOWOTNY, *In Situ* Composites IV, Proceedings MRS Symposium, Vol. 12 (North-Holland, 1983) p. 31.
3. B. D. GRAIG, *Res. Mech. Letters* **8** (1983).
4. *Idem, Scripta Metall.* **15** (1981) 91.
5. M. RAPPOSCH, E. KOSTINER, S. F. WAYNE and H. NOWOTNY, *Mh. Chem.* **116** (1985) 237.
6. E. ERDOS, *Material Technik* **1** (1973) 126.
7. K. LOHBERG and W. SCHMIDT, *Arch. Eisenhuttenw.* **11** (1938) 607.
8. Z. SUN, H. A. DAVIS and J. A. WHITEMAN, *Met. Sci.* **18** (1984) 459.
9. J. C. SCHUSTER and H. NOWOTNY, *Mh. Chem.* **113** (1982) 163.
10. E. I. GLADYSEVSKIJ *et al., Fir. Met. Metalloved* **2** (1956) 454.
11. J. -P. SENATEUR and R. FRUCHART, *Comt. Rend. Acad. Sci. Paris* **258** (1964) 1524.
12. B. ARONSSON, *Acta Chem. Scand.* **12** (1958) 308.
13. K. O. BURGER, *Mh. Chem.* **93** (1962) 9, 674.
14. A. N. KLEIN, R. OBERACKER and F. THUMMLER, Powder Metallurgy Meeting (1984) Karlsruhe FGR.
15. T. SHIGEMATSU *et al., J. Phys. Soc. Jpn* **38** (1975) 1213.
16. H. GUPTA, J. E. MORRAL and H. NOWOTNY, *Scripta Metall.* **20** (1986) 889.
17. H. NOWOTNY and D. D. PEARSON, Final Report (1982/1985) Grant no NAG3-271, NASA Lewis Research Center, Cleveland, Ohio.
18. H. GUPTA, PhD thesis, University of Connecticut (1987).

Received 1 June
and accepted 16 December 1987